Direct momentum-space calculations for the resonant multiphoton processes of a hydrogen atom under intense laser pulses

Ue-Li Pen
Department of Astrophysical Sciences, Princeton University, Princeton, New Jersey 08544-1001

Tsin-Fu Jiang
Institute of Physics, National Chiao Tung University, Hsinchu 30050, Taiwan
(Received 19 April 1995)

We present a momentum-space solution for the time-dependent Schrödinger equation of a realistic hydrogen atom in a strong laser pulse. The method can integrate the nonperturbative system to thousands of optical cycles, previously thought not yet feasible. A hydrogen atom under a 285-nm (4.357-eV), 97.5-TW/cm^2 short pulse is found to produce two prominent photoelectron peaks above threshold, and significant intermediate bound-state resonance with the $4p$ state. With a 248-nm (5-eV) probe laser pulse that is ten times longer, the resonant structure is explored.

PACS number(s): 32.80.Rm, 32.80.Fb, 32.90.+a

The multiphoton excitation of atoms under intense laser fields has been a subject of great interest. Among the studies, most of the experimental works are on rare gas atoms while many theoretical investigations are on the hydrogen atom. The case of atomic hydrogen is of special interest, for there is no electron correlation which complicates the problem. The first above-threshold-ionization (ATI) measurement on the hydrogen atom was in a short-wavelength, long-pulse, and moderate-intensity regime [1]. The progress of laser and experimental technology allows the study of the hydrogen atom in short intense laser fields. Kyrala and Nichols measured the ionization rate of ground-state hydrogen under 248-nm, subpicosecond pulses at TW to 100-TW/cm^2 intensities [2]. Recently, a series of experiments on hydrogen with intense subpicosecond lasers by Feldmann and co-workers have been reported [3–9]. On the theoretical part, Chu and Cooper [10] explained the peak suppression of ATI and branching ratios by Floquet theory. Kulander [11] calculated the multiphoton ionization rate, and Gao and Starace [12] used a variational method to study the two- and three-photon processes in the perturbative regime. The calculations to the 248-nm experiment were tried by LaGattuta [13] and Pindzola and Dörr [14]. Calculations related to Refs. [3–9] were given by Dörr *et al.* [15] and Gontier and Trahin [16].

It is generally believed that the direct solution of the time-dependent Schrödinger equation for this problem has not been feasible yet for a realistic pulse of 1 ps or 100 cycles of field [9,17,18]. The basic difficulty of the calculation is the nonlocalized ionized electronic wave function in the coordinate space. The spreading of a wave packet in space as time passes usually demands a large grid which strains the capacity of even high speed computers. We present in this paper a momentum-space finite element method which enables us to integrate the system easily to thousands of field cycles on a moderate desktop workstation. It generalizes the approaches we developed for the one-dimensional cases [19,20]. A momentum-space approach is ideally suited for problems involving continuum dynamics, since both the bound and the ionized wave functions are localized in momentum space. The wave function thus does not significantly spread in time, making accurate direct calculations tractable. We will employ our method to study the intensity resonance in the multiphoton ionization of hydrogen. This kind of problem on some inert gas atoms has been studied experimentally [21–25]. The mechanism of ionization is not very clear. We will investigate the ionization dynamics with similar conditions imposed on the hydrogen atom and study the excitation mechanisms. It is known that the short laser pulse will expose the resonant structures [26], but we need a longer pulse to resolve the resonances due to the uncertainty principle [21–24]. We propose a numerical experiment with a 285-nm pump laser of 97.5 TW/cm^2, full width at half maximum (FWHM) 400 fs, plus a 248-nm probe laser with ten times longer duration and one-tenth of the intensity. The reasons and results will be explained below.

Let us describe the method first. Consider the integral Schrödinger equation in momentum space,

$$i\hbar \frac{\partial \psi}{\partial t} = \frac{\mathbf{p}^2}{2m_e}\psi + \int V(\mathbf{p},\mathbf{p}',t)\psi(\mathbf{p}')d^3\mathbf{p}'. \tag{1}$$

It can be expanded into piecewise constant basis functions as defined below. To simplify our notation, we use atomic units, where $e=\hbar=m_e=1$. We will use the finite element expansion for the radial momentum coordinate p and expand the angular part as a sum of spherical harmonics,

$$\psi(\mathbf{p}) = \sum_{j,l,m} v_j^{lm}(t)\phi_j(p)Y_{lm}(\theta,\phi). \tag{2}$$

The finite element basis consists of orthonormalized piecewise constant functions:

$$\phi_j(p) = \begin{cases} \dfrac{1}{\sqrt{p_{j+1}-p_j}}, & p_j < p < p_{j+1} \\ 0 & \text{elsewhere.} \end{cases} \tag{3}$$

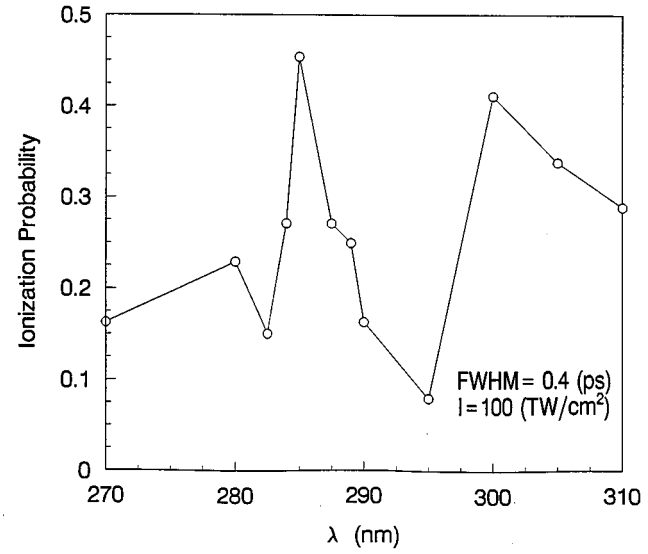

FIG. 1. Ionization probability of hydrogen ground state vs wavelength at fixed laser intensity and fluence.

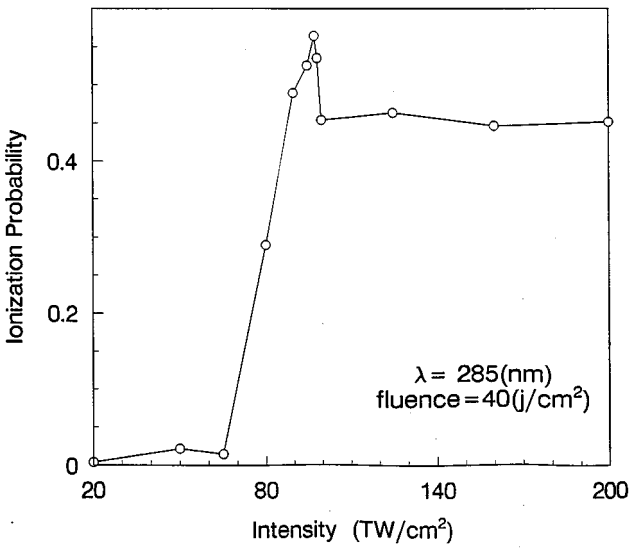

FIG. 2. Ionization probability vs laser intensities at 285 nm and fixed fluence.

Under the dipole approximation and the Coulomb gauge, we obtain an interaction term $\mathbf{A}\cdot\mathbf{p}$. For fields linearly polarized in the z direction, m in (2) is a good quantum number and we drop the index m hereafter.

Substituting (2) into the Schrödinger equation (1), and multiplying by the basis functions Y_{lm} and ϕ_j, we obtain the system of coupled ordinary differential equations

$$i\frac{dv_j^l}{dt}=H_{jk}^l v_k^l+\frac{A(t)p_j}{\sqrt{2l+1}}\left(\frac{v_j^{l+1}}{\sqrt{2l+3}}+\frac{v_j^{l-1}}{\sqrt{2l-1}}\right), \qquad (4)$$

where

$$H_{jk}^l=\int_{p_j}^{p_{j+1}}\left[\frac{p^2}{2}+\int_{p_k}^{p_{k+1}}Q^l\left(\frac{p^2+p'^2}{2pp'}\right)dp'\right]dp. \qquad (5)$$

Here Q^l is the Legendre function of the second kind [27]. We use a staggered leapfrog algorithm to integrate (4) in time [28,29]. For a typical calculation on a workstation, we choose 15 partial waves and 250 momentum elements for each of them. The first 200 momentum elements are uniformly spaced between 0 and 1 a.u., with increasingly wider elements for large p. This grid resolves the ground state accurately and contains enough continuum. Note that the states corresponding to a very high energy will never be populated using the interactions that we study.

In order to find out the resonant condition, we do a simulation of the hydrogen ground state under a short-pulse field $\mathbf{E}(t)=\hat{\mathbf{z}}E_m\sin^2(\pi t/2T_p)\sin(\omega_p t)$, where ω_p is the frequency of the pump laser and T_p is the pulse duration. We keep the laser intensity at 100 TW/cm^2 and FWHM 400 fs. Figure 1 depicts the ionization probability versus laser wavelengths between 270 nm and 310 nm. We find that the maximum ionization occurs around 285 nm, and a local maximum at 300 nm. We will see that the former is due to the enhancement of ionization from a three-photon bound state resonant with a $4p$ state, and the latter is mainly due to a three-photon bound state resonant with a $3p$ state. In the next calculation, we focus the wavelength at 285 nm, and with the same fluence 40 J/cm^2. We scan the intensity between 20 and 200 TW/cm^2; Fig. 2 shows more accurately that the intensity for maximum ionization is 97.5 TW/cm^2. The ionization probability rises quickly near this intensity and is saturated after that. The projections of final-state wave function to the unperturbed eigenstates for some cases are shown in Table I. In

TABLE I. The dominant projection probabilities of the final wave function to the unperturbed eigenstates. The 100-TW/cm^2 case is for 300 nm, the others are for 285-nm cases.

States	$1s$	$3p$	$4p$	$4f$	ϵs	ϵp	ϵd	ϵf	ϵg
65 TW/cm^2	0.977	0.00	0.00	0.00	0.0008	0.0004	0.0076	0.0003	0.0057
	bounded equal to 0.985, ionized equal to 0.015								
97.5 TW/cm^2	0.152	0.00	0.160	0.077	0.076	0.068	0.30	0.0736	0.0431
	bounded equal to 0.436, ionized equal to 0.564								
pump plus probe	0.143	0.00	0.161	0.0823	0.064	0.077	0.30	0.0718	0.0455
	bounded equal to 0.439, ionized equal to 0.561								
100 TW/cm^2	0.406	0.175	0.00	0.00	0.077	0.030	0.12	0.171	0.0143
	bounded equal to 0.587, ionized equal to 0.413								

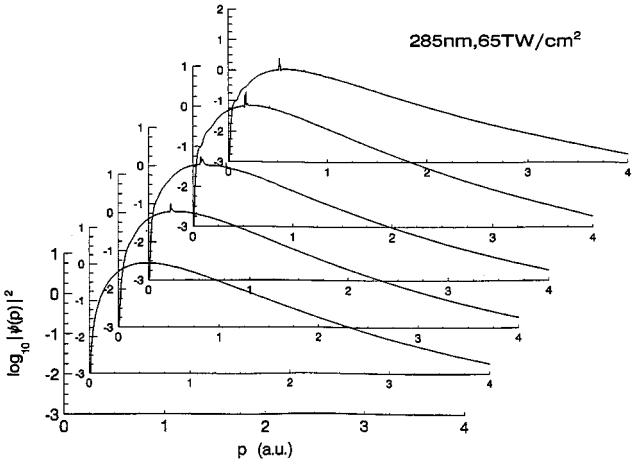

FIG. 3. Time evolution of the radial momentum wave functions. The time from the bottom is 0, 0.2, 0.4, 0.6, 0.8, and 1.0 in T_p, where T_p is the laser duration of pump laser.

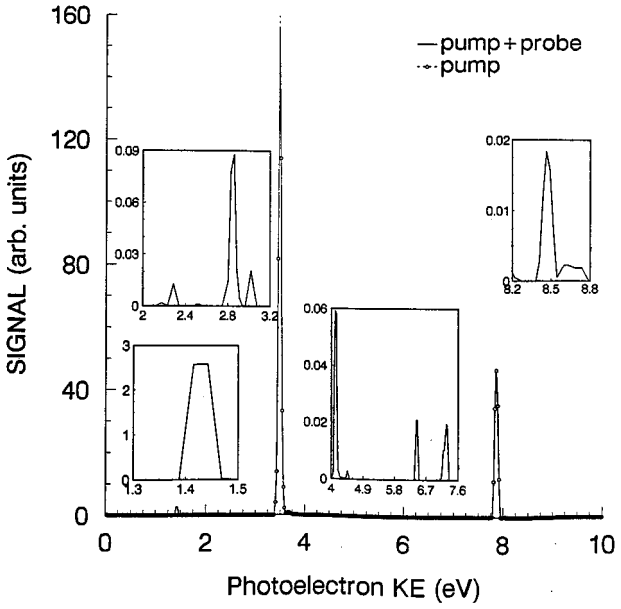

FIG. 5. Photoelectron kinetic energy spectra, the two main ATI peaks are exactly coincident for both the pump and the pump with probe laser cases. The insets are only from pump plus probe excitation. Explanations for the resonances are in the text.

the 285-nm, 97.5-TW/cm^2 case, we can see that there is significant bound-state probability to the $4p$ state. When the $4p$ level is shifted upward by 0.32 eV, it hits the three-photon resonance and is the strongest one among the intermediate resonances. The study shows that a significant fraction of the ionization is resonant and two step in nature. The laser first pumps the electron from the ground state to these bound states via three-photon absorption and then excites it into continuum. For the 65-TW/cm^2 case, the electron remains in the ground state at 98% probability after the excitation. But for the 300-nm, 100-TW/cm^2 case, we found strong bound-state resonance with the $3p$ state. The evidence shows that the intermediate-state resonance enhances the ionization probability and is the dominant process in the ionization mechanisms. The saturation of ionization probability for intensity higher than 97.5 TW/cm^2 is due to the same $4p$ resonance.

Figures 3 and 4 show that the time evolution of wave functions corresponds to the two cases of 285 nm. The spikes correspond to the ATI peaks. But the subpicosecond-pulse duration is too short and not able to resolve the resonances. So we do a further investigation in the 97.5-TW/cm^2 case by an additional probe laser. We choose the probe laser at 248-nm, 4-ps FWHM at an intensity of 9.75 TW/cm^2. The electric field shape is $\sin^2(\pi t/2T_b)\sin(\omega_b t)$, where ω_b is the frequency of the probe laser. The probe laser pulse duration T_b is ten times longer than T_p, and the one-tenth intensity makes ponderomotive effect negligible. *Note that the pulse duration is 6820 times the laser period. It is far beyond the mentioned calculation bottleneck of 100 field cycles* [9,17,18]. The projection of the final wave function to unperturbed eigenstates is shown in Table I. It is most likely the same as the 97.5-TW/cm^2 pump case as expected because the additional probe laser intensity is weak. But the photoelectron energy resolution is much improved.

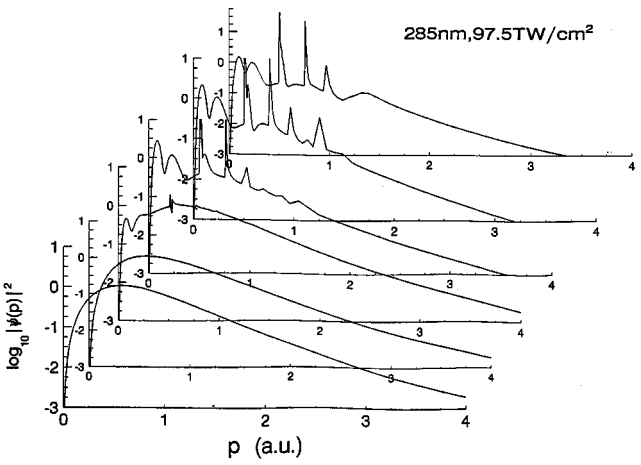

FIG. 4. The same as Fig. 3 but for resonant intensity.

We show in Fig. 5 the photoelectron spectra of the case with pump laser only, and with additional probe laser case. The former case resolves only two dominant ATI peaks at 3.48 and 7.86 eV that are exactly coincident with the latter case. They originate from four- and five-photon ionization of pump laser photons. The insets in Fig. 5 are from the probe laser only. The peaks are at the photoelectron energies 1.43, 2.3, 2.86, 3.02, 4.12, 4.46, 6.43, 7.3, and 8.46 eV. The peaks come from $3\hbar\omega_b - V_{\rm ion} = 1.4$, $E_{n=4} + \hbar\omega_b = 4.15$, $E_{n=5} + \hbar\omega_b = 4.456$, $4\hbar\omega_b - V_{\rm ion} = 6.4$, $E_{n=3} + 2\hbar\omega_b = 8.49$. The resonant peak $E_{n=3} + \hbar\omega_b = 3.49$ happens to be coincident with the first main ATI peak and cannot be resolved. $V_{\rm ion}$ is the ionization potential of the hydrogen atom, which is 13.6 eV. The peak at 2.86 eV is from $E_{n=3} + \hbar\omega_p = 2.85$. From the analysis of angular momentum, we believe that the peaks at 2.3 and 3.02 eV are from pon-

deromotive shifted weak resonances of $E_{n=3}+\hbar\omega_p$. The resonance at 7.3 eV is obviously from $2.3+\hbar\omega_b$. We can see that the probe laser exposes the resonances clearly.

In summary, our momentum-space finite element method enables us to analyze the detailed mechanism of strong field ionization for a real hydrogen atom. Calculations of this kind can now be pushed to thousands of optical cycles. The designed pump plus probe laser excitation should be interesting in this field. We plan to publish further details of our method and study on other topics elsewhere.

This work was supported by National Science Council, Taiwan under Contract No. NSC85-2112-M-009-005. We are grateful for the very helpful comments from Professor A.F. Starace and Professor Shih-I Chu.

[1] H.G. Muller, H.B. van Linden, and M.J. van der Wiel, Phys. Rev. A **34**, 236 (1986).
[2] G.A. Kyrala and T.D. Nichols, Phys. Rev. A **44**, R1450 (1991).
[3] B. Wolff, H. Rottke, D. Feldmann, and K.H. Welge, Z. Phys. D **10**, 35 (1988).
[4] H. Rottke, B. Wolff, M. Brickwedde, D. Feldmann, and K.H. Welge, Phys. Rev. Lett. **64**, 404 (1990).
[5] D. Feldmann, Comments At. Mol. Phys. **24**, 311 (1990).
[6] Y. Gontier, M. Trahin, B. Wolff-Rottke, H. Rottke, K.H. Welge, and D. Feldmann, Phys. Rev. A **46**, 5594 (1992).
[7] M. Dörr, D. Feldmann, R.M. Potvliege, H. Rottke, R. Shakeshaft, K.H. Welge, and B. Wolff-Rottke, J. Phys. B **25**, L275 (1992).
[8] H. Rottke, D. Feldmann, B. Wolff-Rottke, and K.H. Welge, J. Phys. B **26**, L15 (1993).
[9] H. Rottke, B. Wolff-Rottke, D. Feldmann, K.H. Welge, M. Dörr, R.M. Potvliege, and R. Shakeshaft, Phys. Rev. A **49**, 4837 (1994).
[10] S.-I. Chu and J. Cooper, Phys. Rev. A **32**, 2769 (1985).
[11] K.C. Kulander, Phys. Rev. A **35**, 445 (1987).
[12] Bo Gao and A.F. Starace, Phys. Rev. Lett. **61**, 404 (1988); Phys. Rev. A **39**, 4550 (1989).
[13] K.J. LaGattuta, Phys. Rev. A **41**, 5110 (1990); **47**, 1560 (1993).
[14] M.S. Pindzola and M. Dörr, Phys. Rev. A **43**, 439 (1991).
[15] M. Dörr, R.M. Potvliege, and R. Shakeshaft, Phys. Rev. A **41**, 558 (1990).
[16] Y. Gontier and M. Trahin, Phys. Rev. A **46**, 1488 (1992).
[17] R.R. Freeman and P.H. Bucksbaum, J. Phys. B **24**, 325 (1991).
[18] K. Burnett, V.C. Reed, and P.L. Knight, J. Phys. B **26**, 561 (1993).
[19] Ue-Li Pen and T.F. Jiang, Phys. Rev. A **46**, 4297 (1992).
[20] T.F. Jiang, Phys. Rev. A **48**, 3995 (1993).
[21] M.P. de Boer and H.G. Muller, Phys. Rev. Lett. **68**, 2647 (1992).
[22] G.N. Gibson, R.R. Freeman, and T.J. McIlrath, Phys. Rev. Lett. **69**, 1904 (1992).
[23] M.P. de Boer, L.D. Noordam, and H.G. Muller, Phys. Rev. A **47**, 45 (1993).
[24] R.B. Vrijen, J.H. Hoogenraad, H.G. Muller, and L.D. Noordam, Phys. Rev. Lett. **70**, 3016 (1993).
[25] R.B. Vrijen, J.H. Hoogenraad, and L.D. Noordam, Mod. Phys. Lett. B **4**, 205 (1994).
[26] R.R. Freeman, P.H. Bucksbaum, H. Milchberg, S. Darack, D. Schumacher, and M.E. Geusic, Phys. Rev. Lett. **59**, 1092 (1987).
[27] S. Flügge, *Practical Quantum Mechanics* (Springer-Verlag, Berlin, 1971).
[28] W.H. Press, S.A. Teukolsky, W.T. Vetterling, and B.P. Flannery, *Numerical Recipes in Fortran*, 2nd ed. (Cambridge University Press, Cambridge, England, 1992).
[29] T.F. Jiang and J.M. Yuan, Int. J. Quantum Chem. Symp. **28**, 65 (1994).